GSA Data Repository Item 2015098

Kikiktat Volcanics of Arctic Alaska – Melting of harzburgitic mantle associated with the Franklin Large Igneous Province

Grant M. Cox[1*], Justin V. Strauss[2], Galen P. Halverson[1], Mark D. Schmitz[3], William C. McClelland[4], Ross S. Stevenson[5] and Francis A. Macdonald[2]

1 - McGill University, Montréal, Québec, Canada.
2 - Harvard University, Cambridge, Massachusetts, U.S.A.
3 – Boise State University, Boise, Idaho, U.S.A.
4 - University of Iowa, Iowa City, Il, U.S.A.
5 - L'Université du Québec à Montréal, Montreal, Quebec, Canada.

Sample Selection

All samples where obtained from outcrop within the measured sections with the base at N69 32'46.5" W146 03'54.7" and the top at N69 32'23.6" W146 03'52.0". All samples chosen for analysis was done after thorough petrographic analysis and selected so as to avoid samples that exhibited extensive alteration.

Analytical Methods

XRF Analysis:

Rock samples were first trimmed to remove weathered surfaces and then cut into ~5 cm^3 fragments using a diamond-bladed rock saw. The rocks were crushed to rock chips in an iron jaw crusher. The chips where milled in a tungsten carbide mill until the powder could pass through a 75 µm mesh. Major and trace element abundances were analyzed by X-ray fluorescence using a Philips PW2400 4kW automated XRF spectrometer system with a rhodium 60 kV end window X-ray tube. Major elements, Cr, Ni and V were analyzed using 32 mm diameter fused beads prepared from a 1:5 sample/lithium tetraborate mixture. Sc, Rb, Sr, Zr, Nb and Y were analyzed using 40 mm diameter pressed pellets prepared at a pressure of 20 tons from a mixture of 10 g sample powder with 2 g Hoechst Wax C Micropowder. Calibration regression lines were prepared using between 15 and 40 International Standard Reference Materials. Corrections for mass absorption effects were applied on concentration values using a combination of alpha coefficients and/or Compton scatter. The accuracy for silica is within 0.5% absolute, and is within 1% for other majors and within 5% for trace elements. Instrument precision is within 0.3% relative, generally within 0.23% relative, and the overall precision for beads and pressed pellets is within 0.5% relative. Results can be found in the electronic supplementary material (Table S1).

Trace Element Analysis:

Rock samples were first trimmed to remove weathered surfaces and then cut into ~5 cm^3 fragments using a diamond-bladed rock saw. The rocks were crushed to rock chips in an iron jaw crusher. The chips where milled in a tungsten carbide mill until the powder could pass through a 75 µm mesh. The resulting powder was weighed (~0.02 g) into cleaned teflon bombs and dissolved under pressure with a HF-HNO_3 mixture. The resulting solutions were evaporated and dissolved again in perchloric acid to facilitate conversion of

fluoride salts to chloride salts. The samples were then dissolved in aqua-regia followed by 6N HCl then finally in 6N HNO_3. The resulting material was redissolved in 5% HNO_3 and analysised for trace elements on a Perkins Elmer quadruple ICP-MS. Full results are shown in Table SX. Results can be found in the electronic supplementary material (Table S1).

Sm-Nd Isotopic Analysis:

Sm and Nd concentrations reported in Table SX were determined by isotope dilution. Approximately ~ 0.3 g of sample powder was spiked with enriched ^{150}Nd-^{149}Sm tracers and dissolved under pressure with a HF-HNO_3 mixture in Teflon containers. The resulting solutions were evaporated and dissolved again in perchloric acid to facilitate conversion of fluoride salts to chloride salts. The samples were then dissolved in aqua-regia followed by 6N HCl. Nd and Sm were extracted using a three stage-chemistry procedure. The first stage involved the removal of Fe by passing the sample through columns filled with 200-400 mesh AG1X8 anion exchange resin. Subsequent to the removal of Fe, the REE component was concentrated using columns filled with Eichrom TRU Resin SPS 50-100μm. The third stage purification of the Sm and Nd fractions entailed passing the samples through columns filled with 600 mg of Eichrom LN Resin 100-150 μm.

The $^{143}Nd/^{144}Nd$ and $^{147}Sm/^{144}Nd$ ratios reported were measured on a Thermo Triton mass spectrometer in the GEOTOP laboratories at Université du Québec à Montréal. Nd and Sm were analyzed using a double filament array with the samples loaded onto outgassed Re filaments, parallel to this was an outgassed Re ionization filament. Nd and Sm samples were measured in dynamic mode, the total combined blank for Sm and Nd is less than 150 pg. The reported Sm and Nd concentrations and the $^{147}Sm/^{144}Nd$ ratios have less than 0.5% error, corresponding to an error of less than 0.5 ε_{Nd} unit for the initial Nd isotopic composition. $^{146}Nd/^{144}Nd$ was normalized to 0.7219 for mass fractionation corrections. Repeated measurements of JNdi-1 standard yielded a value of $^{143}Nd/^{144}Nd = 512109 \pm 1$ (n =20) for the period of the study. This value is within error of the value obtained by Tanaka et al. (2000) of $^{143}Nd/^{144}Nd = 0.512115 \pm 7$. Repeated measurements of BHVO-2 yielded a value of $^{143}Nd/^{144}Nd = 0.512965 \pm 6$ (n = 20) for the period of the study. This value is within error of the accepted value of $^{143}Nd/^{144}Nd = 0.51298 \pm 12$ (Jochum et al., 2005). The chondritic reference values used for ε_{Nd} calculations are; $^{143}Nd/^{144}Nd_{CHUR} = 0.512636$, $^{147}Sm/^{144}Nd_{CHUR} = 0.1966$, and the decay constant for ^{147}Sm was assumed to be 6.54 x 10-12 a^{-1}.

U-Pb Isotopic Analysis:

Heavy mineral separates containing populations of moderate to highly elongated, prismatic zircon crystals were separated by conventional density and magnetic methods. The bulk zircon separates for each sample were placed in a muffle furnace at 900°C for 60 hours in quartz beakers to anneal minor radiation damage; annealing enhances cathodoluminescence (CL) emission, promotes more reproducible inter element fractionation during laser ablation inductively coupled plasma mass spectrometry (LA-ICPMS), and prepares the crystals for subsequent chemical abrasion (Mattinson, 2005).

Zircons were analyzed by laser ablation multicollector inductively coupled plasma mass spectrometry (LA-MC-ICPMS) at the Arizona LaserChron Center using a Photon Machines Analyte G2 excimer laser coupled with a Nu HR ICPMS following protocols of Gehrels et al. (2006; 2008). Measurements were made in static mode, using Faraday detectors with $3x10^{11}$

ohm resistors for ^{238}U, ^{232}Th, ^{208}Pb-^{206}Pb, and discrete dynode ion counters for ^{204}Pb and ^{202}Hg. Ion yields are ~0.8 mv per ppm. Each analysis implemented a 15-second laser-absent integration for for backgrounds followed by 15 one-second integrations with the laser firing and a final 30 second delay to purge the previous sample and prepare for the next analysis. Analyses used a spot diameter of 30 microns and ablation pit depth of ~15 microns. Measurement errors for each analysis resulted in ~1-2% (at 2-sigma level) uncertainty in the $^{206}Pb/^{238}U$ and $^{206}Pb/^{207}Pb$ ages, with the uncertainty in the $^{206}Pb/^{207}Pb$ age increasing for younger grains due to lower abundance of ^{207}Pb. Interference of ^{204}Hg with ^{204}Pb was subtracted using the measured ^{202}Hg and natural $^{202}Hg/^{204}Hg$ ratio of 4.35. Common Pb correction used the Hg-corrected ^{204}Pb and initial common Pb composition from Stacey and Kramers (1975) with uncertainties of 1.5 for $^{206}Pb/^{204}Pb$ and 0.3 for $^{207}Pb/^{204}Pb$. Inter-element fractionation and U-Th concentrations were established by analysis of natural Sri Lanka zircon standard (563.5 ± 3.2 Ma (2-sigma error), ~518 ppm U, 68 ppm Th; (Gehrels et al., 2008)) between every 5 unknowns.

All U-Pb isotopic analyses via chemical abrasion isotope dilution thermal ionization mass spectrometry (CA-IDTIMS) were undertaken on crystals previously mounted, polished and selected on the basis of LA-ICPMS analysis. Crystals were plucked from grain mounts, chemically abraded using a single aggressive abrasion step in concentrated HF at 195°C for 12 hours, and the residual crystals processed for isotope dilution thermal ionization mass spectrometry (ID-TIMS). The details of ID-TIMS analysis are described by Davydov et al. (2010) and Schmitz and Davydov (2012). U-Pb dates and uncertainties for each analysis were calculated using the algorithms of Schmitz and Schoene (2007), the U decay constants of Jaffey et al. (1971), and values of $^{235}U/^{205}Pb$ = 100.2329 and $^{233}U/^{235}U$ = 0.99506 for the ET535. Other details of analytical parameters can be found in the notes to Table DR1. The quoted uncertainties in Table DR1 are based upon non-systematic analytical errors, including counting statistics, instrumental fractionation, tracer subtraction, and blank subtraction. These error estimates should be considered when comparing our $^{206}Pb/^{238}U$ dates with those from other laboratories that used tracer solutions calibrated against the EARTHTIME gravimetric standards. When comparing our dates with those derived from other decay schemes (e.g., $^{40}Ar/^{39}Ar$, ^{187}Re-^{187}Os), the uncertainties in tracer calibration (0.05%;(Condon et al., 2007)) and U decay constants (0.108%;(Jaffey et al., 1971)) should be added to the internal error in quadrature. Sample ages are thus reported as ± X (Y) [Z] Ma, where X is the internal error, Y is the internal plus tracer calibration error, and Z is the internal plus tracer plus decay constant uncertainty.

Statistical Modeling

Principal Component Analysis

Principal component analysis is designed to determine the direction(s) of maximum variance within a data set. In effect what PCA achieves is to take a large multi-variant dataset and rotate it so that the maximum variability is visible, consequently identifying the most important gradients. The basic steps involved in PCA are:

1. Dataset centering: this step centers the data set as a whole to zero while maintaining the relative distance between the individual data points.
2. Covariance of the data points is calculated and a covariance matrix established.
3. Eigenvectors (direction of variance) and eigenvalues fro the matrix are calculated (amount of variance).

4. Components of significance are chosen and those components that contribute little to the overall variance are discarded, this in effect reduces the dimensionality of the original data set.
5. Utilizing the chosen feature vectors original data is transformed so that it is expressed solely in terms of the principal components of significance.

Unlike other statistical and graphical techniques of data analysis PCA results in the quantification (factor loadings) of the contribution of the variables to the direction of maximum variation(s) (principal component(s)). Like many statistical techniques PCA is susceptible to issues of scale, this may seem a serious issue when applied to geochemical data where the variables may be expressed in ppm and weight percent levels, implying ~6 order of magnitude difference in scale. However, it is important to note that scale issues are only apparent on absolute values, PCA neither requires nor cares about units, consequently issues surrounding ppm and weight percent data are in most cases spurious.

Principal component analysis was undertaken using the XLSTAT™ program. Full results are shown in Table 7. For further information on PCA the reader is referred to Wold et al. (1987) and references within.

alphaMELTS Modeling

For full details of the alphaMELTS modeling software the reader is referred to Ghiroso & Sack (1995), Asimow & Ghiorso (1998), and Ghiorso et al. (2002).

Fractional Crystallization Models:

All isobaric fractional crystallization models were conducted at pressures of 1 kb (other pressures were used but discarded due to incompatibility with the observed liquid line of descent) utilizing the MELTS thermodynamic model. Delta T was set at -0.5°C and fO_2 was fixed at FMQ, all models were initiated at their respective liquidus temperatures. When trace element data is included, partition co-efficients are from McKenzie & O'Nions (1991) and do not vary during the course of each model run. The composition used in these calculations is that of the sample with highest MgO, its normative and major element composition is shown in Table S4.

Phase Diagram Construction:
Phase diagrams were constructed by using composition of the parental melt (Table S4) with multiple model runs at varying pressures to construct a pressure-temperature grid. For each model run delta T was set at -0.5°C and fO_2 was set at FMQ.

Mg8.0 Analysis

The use of $MgO_{8.0}$ is well a documented method to recalculate lava compositions either back or forward to are standard value of 8% MgO. Originally developed for use on oceanic basalts (Klein and Langmuir, 1987) and subsequently adapted specifically for continental flood basalts (Turner and Hawkesworth, 1995). The goal of this method is to be able compare disparate lava compositions at a similar point in their petrogenesis, as MgO has a strong linear relationship to temperature (e.g (Niu et al., 2002)), MgO is the basis of

the recalculation. While the choice of 8% MgO is a somewhat arbitrary but widely used comparison point it does broadly coincide with liquids hitting the olivine-plagioclase-clinopyroxene cotectic, consequently typically two linear regressions (either side of 8% MgO) can be undertaken to adjust compositions back to 8% MgO. These back calculations should not be confused with forward and/or reverse fractional crystallization methods (i.e. (Danyushevsky and Plechov, 2011) which assume and/or estimate phase proportions. Compositions in $MgO_{8.0}$ analysis are recalculated using equations of curves fitted to the data (typically least squared regressions), consequently this type of analysis neither assumes nor requires the phase proportions associated with the crystallizing assemblage. Another benefit of this method lacking from typical forward and back calculations that rely of phase proportions is that since assimilation is generally coupled to fractional crystallization (Cribb and Barton, 1996; DePaolo, 1981) this method accounts for the affects of contamination.

References

Asimow, P. D., and Ghiorso, M. S., 1998, Algorithmic modifications extending MELTS to calculate subsolidus phase relations: American Mineralogist, v. 83, no. 9-10, p. 1127-1132.

Condon, D., Schoene, B., Bowring, S., Parrish, R., McLean, N., and Crowley, Q., 2007, EARTHTIME; isotopic tracers and optimized solutions for high-precision U-Pb ID-TIMS geochronology: Eos, Transactions, American Geophysical Union., v. 88, no. 52.

Cribb, J. W., and Barton, M., 1996, Geochemical effects of decoupled fractional crystallization and crustal assimilation: Lithos, v. 37, no. 4, p. 293-307.

Danyushevsky, L. V., and Plechov, P., 2011, Petrolog3: Integrated software for modeling crystallization processes: Geochemistry, Geophysics, Geosystems, v. 12, no. 7, p. Q07021.

Davydov, V. I., Crowley, J. L., Schmitz, M. D., and Poletaev, V. I., 2010, High-precision U-Pb zircon age calibration of the global Carboniferous time scale and Milankovitch-band cyclicity in the Donets Basin, eastern Ukraine: Geochemistry, Geophysics, Geosystems, v. 11.

DePaolo, D. J., 1981, Trace element and isotopic effects of combined wallrock assimilation and fractional crystallization: Earth and Planetary Science Letters, v. 53, no. 2, p. 189-202.

Gehrels, G. E., Valencia, V., and Pullen, A., 2006, Detrital zircon geochronology by Laser-Ablation Multicollector ICPMS at the Arizona LaserChron Center, *in* Loszewski, T., and Huff, W., eds., Geochronology: Emerging Opportunities, Paleontology Society Short Course, Volume v. 11, Paleontology Society Papers, p. 10.

Gehrels, G. E., Valencia, V., and Ruiz, J., 2008, Enhanced precision, accuracy, efficiency, and spatial resolution of U-Pb ages by laser ablation-multicollector-inductively coupled plasma-mass spectrometry: Geochemistry, Geophysics, Geosystems, v. 9.

Ghiorso, M. S., Hirschmann, M. M., Reiners, P. W., and Kress, V. C., III, 2002, The pMELTS: A revision of MELTS for improved calculation of phase relations and major element partitioning related to partial melting of the mantle to 3 GPa: Geochem. Geophys. Geosyst., v. 3, no. 5, p. 1030.

Ghiorso, M. S., and Sack, R. O., 1995, Chemical mass transfer in magmatic processes IV. A revised and internally consistent thermodynamic model for the interpolation and extrapolation of liquid-solid equilibria in magmatic systems at elevated temperatures and pressures: Contributions to Mineralogy and Petrology, v. 119, no. 2, p. 197-212.

Jaffey, A. H., Flynn, K. F., Glendenin, L. E., Bentley, W. C., and Essling, A. M., 1971, Precision measurements of half-lives and specific activities of 235U and 238U: Physical Review, v. C, no. 4, p. 1889-1906.

Jochum, K. P., Nohl, U., Herwig, K., Lammel, E., Stoll, B., and Hofmann, A. W., 2005, GeoReM: A New Geochemical Database for Reference Materials and Isotopic Standards: Geostandards and Geoanalytical Research, v. 29, no. 3, p. 333-338.

Klein, E. M., and Langmuir, C. H., 1987, Global Correlations of Ocean Ridge Basalt Chemistry with Axial Depth and Crustal Thickness: Journal of Geophysical Research, v. 92, no. B8, p. 8089-8115.

Mattinson, J. M., 2005, Zircon U-Pb chemical abrasion ("CA-TIMS") method: combined annealing and multi-step partial dissolution analysis for improved precision and accuracy of zircon ages: Chemical Geology, v. 220, p. 47-66.

McKenzie, D. A. N., and O'Nions, R. K., 1991, Partial Melt Distributions from Inversion of Rare Earth Element Concentrations: Journal of Petrology, v. 32, no. 5, p. 1021-1091.

Niu, Y., Gilmore, T., Mackie, S., Greig, A., and Bach, W., 2002, Mineral chemistry, whole rock compositions and petrogenesis of leg 176 gabbros: Data and Discussion, *in* Natland, J. H., Dic, H. J. B., Miller, D. J., and Von Herzen, R. P., eds., Proceedings of the Ocean Drilling Program, Scientific Results, Volume 176.

Schmitz, M. D., and Davydov, V. I., 2012, Quantitative radiometric and biostratigraphic calibration of the global Pennsylvanian – Early Permian time scale: Geological Society of America Bulletin, v. 124, p. 549-577.

Schmitz, M. D., and Schoene, B., 2007, Derivation of isotope ratios, errors and error correlations for U-Pb geochronology using 205Pb-235U-(233U)-spiked isotope dilution thermal ionization mass spectrometric data: Geochemistry, Geophysics, Geosystems, v. 8.

Stacey, J. S., and Kramers, J. D., 1975, Approximation of terrestrial lead isotope evolution by a two stage model: Earth and Planetary Science Letters, v. 26, p. 207-221.

Tanaka, T., Togashi, S., Kamioka, H., Amakawa, H., Kagami, H., Hamamoto, T., Yuhara, M., Orihashi, Y., Yoneda, S., Shimizu, H., Kunimaru, T., Takahashi, K., Yanagi, T., Nakano, T., Fujimaki, H., Shinjo, R., Asahara, Y., Tanimizu, M., and Dragusanu, C., 2000, JNdi-1: a neodymium isotopic reference in consistency with LaJolla neodymium: Chemical Geology, v. 168, no. 3-4, p. 279-281.

Turner, S., and Hawkesworth, C., 1995, The nature of the sub-continental mantle: constraints from the major-element composition of continental flood basalts: Chemical Geology, v. 120, no. 3-4, p. 295-314.

Wold, S., Esbensen, K., and Geladi, P., 1987, Principal component analysis: Chemometrics and Intelligent Laboratory Systems, v. 2, no. 1–3, p. 37-52.

Table DR1. Principal component anaysis

Summary statistics:

Variable	Observations	Minimum	Maximum	Mean	Std. deviation
eNd(T)	20	-12.208	3.915	-5.898	4.100
SiO2	20	48.710	51.559	50.190	0.914
TiO2	20	0.829	2.831	1.310	0.460
Al2O3	20	11.930	16.663	14.968	1.095
FeOT	20	9.897	17.557	12.367	1.999
MgO	20	4.674	11.834	7.981	1.866
CaO	20	6.909	10.774	8.958	1.239
Total Alkalis	20	2.201	4.961	3.700	0.979
Total LILE	20	95.466	596.420	225.163	146.238
Total HFS	20	47.698	183.974	97.207	35.191
Total HREE	20	10.145	26.593	15.186	3.910
Total LREE	20	32.953	82.912	52.358	14.722
LREE/HREE	20	2.148	4.712	3.478	0.661

Correlation matrix (Pearson (n)):

Variables	eNd(T)	SiO2	TiO2	Al2O3	FeOT	MgO	CaO	Total Alkalis	Total LILE	Total HFS	Total HREE	Total LREE	LREE/HREE
eNd(T)	**1**	-0.314	0.341	**-0.547**	0.417	0.152	-0.247	-0.097	-0.341	0.022	0.327	-0.231	**-0.751**
SiO2	-0.314	**1**	0.352	-0.357	0.295	**-0.617**	-0.303	0.218	0.330	**0.610**	**0.540**	**0.706**	0.342
TiO2	0.341	0.352	**1**	**-0.762**	**0.840**	**-0.686**	-0.359	0.017	-0.308	**0.889**	**0.925**	**0.713**	-0.122
Al2O3	**-0.547**	-0.357	**-0.762**	**1**	**-0.875**	**0.499**	0.383	-0.010	0.277	**-0.645**	**-0.834**	**-0.508**	0.311
FeOT	0.417	0.295	**0.840**	**-0.875**	**1**	**-0.734**	**-0.572**	0.309	-0.230	**0.795**	**0.869**	**0.640**	-0.174
MgO	0.152	**-0.617**	**-0.686**	**0.499**	**-0.734**	**1**	0.382	**-0.467**	-0.113	**-0.879**	**-0.792**	**-0.805**	-0.165
CaO	-0.247	-0.303	-0.359	0.383	**-0.572**	0.382	**1**	**-0.766**	-0.200	-0.412	-0.418	-0.388	-0.008
Total Alkalis	-0.097	0.218	0.017	-0.010	0.309	**-0.467**	**-0.766**	**1**	**0.473**	0.220	0.171	0.214	0.069
Total LILE	-0.341	0.330	-0.308	0.277	-0.230	-0.113	-0.200	**0.473**	**1**	-0.099	-0.133	0.048	0.250
Total HFS	0.022	**0.610**	**0.889**	**-0.645**	**0.795**	**-0.879**	-0.412	0.220	-0.099	**1**	**0.906**	**0.908**	0.173
Total HREE	0.327	**0.540**	**0.925**	**-0.834**	**0.869**	**-0.792**	-0.418	0.171	-0.133	**0.906**	**1**	**0.747**	-0.185
Total LREE	-0.231	**0.706**	**0.713**	**-0.508**	**0.640**	**-0.805**	-0.388	0.214	0.048	**0.908**	**0.747**	**1**	**0.509**
LREE/HREE	**-0.751**	0.342	-0.122	0.311	-0.174	-0.165	-0.008	0.069	0.250	0.173	-0.185	**0.509**	**1**

Values in bold are different from 0 with a significance level alpha=0.05

Bartlett's sphericity test:

Chi-square (Observed value)	-Inf
Chi-square (Critical value)	99.617
DF	78
alpha	0.05

Test interpretation:
H0: There is no correlation significantly different from 0 between the variables.
Ha: At least one of the correlations between the variables is significantly different from 0.

Principal Component Analysis:

Eigenvalues:

	F1	F2	F3	F4	F5	F6	F7	F8	F9	F10	F11	F12	F13
Eigenvalue	6.392	2.898	1.728	0.739	0.508	0.323	0.238	0.094	0.041	0.021	0.017	0.001	0.000
Variability (%)	49.173	22.292	13.293	5.687	3.905	2.487	1.833	0.721	0.315	0.159	0.127	0.009	0.000
Cumulative %	49.173	71.464	84.757	90.444	94.349	96.836	98.669	99.389	99.705	99.864	99.991	100.000	100.000

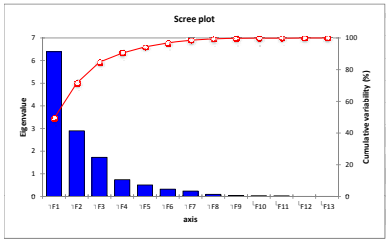

Eigenvectors:

	F1	F2	F3	F4	F5	F6	F7	F8	F9	F10	F11	F12	F13
eNd(T)	0.077	0.509	0.236	0.104	0.262	0.236	0.156	0.707	-0.092	-0.096	0.002	-0.042	0.004
SiO2	0.239	-0.305	-0.090	0.499	0.328	-0.566	0.126	0.144	-0.233	-0.098	-0.010	-0.006	0.253
TiO2	0.353	0.157	-0.157	-0.063	-0.077	0.262	0.410	-0.361	-0.257	-0.567	0.106	-0.160	0.157
Al2O3	-0.316	-0.261	0.019	-0.173	-0.304	0.046	0.599	0.211	-0.200	0.172	-0.370	0.127	0.285
FeOT	0.360	0.160	0.087	-0.173	-0.045	0.100	-0.446	-0.081	-0.351	0.272	-0.275	0.119	0.550
MgO	-0.342	0.173	0.011	-0.024	0.526	0.081	0.175	-0.287	0.350	0.113	0.177	0.068	0.534
CaO	-0.225	0.063	-0.522	0.309	-0.426	0.120	-0.263	0.275	0.169	-0.194	0.167	-0.042	0.375
Total Alkalis	0.131	-0.236	0.605	-0.226	-0.267	-0.186	-0.064	0.156	0.322	-0.318	0.269	-0.052	0.308
Total LILE	-0.028	-0.376	0.358	0.570	0.008	0.612	-0.059	-0.124	-0.071	0.075	0.014	-0.018	0.002
Total HFS	0.376	-0.069	-0.152	-0.057	-0.129	0.081	0.265	0.106	-0.001	0.569	0.632	-0.005	0.020
Total HREE	0.378	0.106	-0.052	0.190	-0.105	0.031	0.157	-0.038	0.464	-0.045	-0.244	0.699	-0.058
Total LREE	0.336	-0.234	-0.209	-0.113	0.157	0.164	0.040	0.138	0.467	0.094	-0.405	-0.558	0.051
LREE/HREE	0.008	-0.477	-0.258	-0.391	0.376	0.278	-0.172	0.263	-0.122	-0.254	0.147	0.366	-0.028

Factor loadings:

	F1	F2	F3	F4	F5	F6	F7	F8	F9	F10	F11	F12	F13
eNd(T)	0.195	0.867	0.310	0.090	0.187	0.134	0.076	0.216	-0.019	-0.014	0.000	-0.001	0.000
SiO2	0.605	-0.519	-0.118	0.429	0.234	-0.322	0.061	0.044	-0.047	-0.014	-0.001	0.000	0.001
TiO2	0.892	0.268	-0.206	-0.054	-0.055	0.149	0.200	-0.111	-0.052	-0.082	0.014	-0.005	0.001
Al2O3	-0.799	-0.444	0.024	-0.149	-0.217	0.026	0.293	0.065	-0.040	0.025	-0.048	0.004	0.001
FeOT	0.911	0.273	0.114	-0.149	-0.032	0.057	-0.218	-0.025	-0.071	0.039	-0.035	0.004	0.003
MgO	-0.865	0.295	0.015	-0.021	0.375	0.046	0.085	-0.088	0.071	0.016	0.023	0.002	0.002
CaO	-0.569	0.107	-0.687	0.265	-0.304	0.068	-0.128	0.084	0.034	-0.028	0.021	-0.001	0.002
Total Alkalis	0.330	-0.402	0.796	-0.195	-0.190	-0.106	-0.031	0.048	0.065	-0.046	0.035	-0.002	0.001
Total LILE	-0.070	-0.640	0.471	0.490	0.005	0.348	-0.029	-0.038	-0.014	0.011	0.002	-0.001	0.000
Total HFS	0.950	-0.117	-0.200	-0.049	-0.092	0.046	0.129	0.032	0.000	0.082	0.081	0.000	0.000
Total HREE	0.956	0.181	-0.069	0.163	-0.075	0.017	0.076	-0.012	0.094	-0.007	-0.031	0.024	0.000
Total LREE	0.849	-0.398	-0.275	-0.097	0.112	0.093	0.020	0.042	0.094	0.014	-0.052	-0.019	0.000
LREE/HREE	0.021	-0.812	-0.339	-0.336	0.268	0.158	-0.084	0.080	-0.025	-0.037	0.019	0.013	0.000

Correlations between variables and factors:

	F1	F2	F3	F4	F5	F6	F7	F8	F9	F10	F11	F12	F13
eNd(T)	0.195	0.867	0.310	0.090	0.187	0.134	0.076	0.216	-0.019	-0.014	0.000	-0.001	0.000
SiO2	0.605	-0.519	-0.118	0.429	0.234	-0.322	0.061	0.044	-0.047	-0.014	-0.001	0.000	0.001
TiO2	0.892	0.268	-0.206	-0.054	-0.055	0.149	0.200	-0.111	-0.052	-0.082	0.014	-0.005	0.001
Al2O3	-0.799	-0.444	0.024	-0.149	-0.217	0.026	0.293	0.065	-0.040	0.025	-0.048	0.004	0.001
FeOT	0.911	0.273	0.114	-0.149	-0.032	0.057	-0.218	-0.025	-0.071	0.039	-0.035	0.004	0.003
MgO	-0.865	0.295	0.015	-0.021	0.375	0.046	0.085	-0.088	0.071	0.016	0.023	0.002	0.002

CaO	-0.569	0.107	-0.687	0.265	-0.304	0.068	-0.128	0.084	0.034	-0.028	0.021	-0.001	0.002
Total Alkalis	0.330	-0.402	0.796	-0.195	-0.190	-0.106	-0.031	0.048	0.065	-0.046	0.035	-0.002	0.001
Total LILE	-0.070	-0.640	0.471	0.490	0.005	0.348	-0.029	-0.038	-0.014	0.011	0.002	-0.001	0.000
Total HFS	0.950	-0.117	-0.200	-0.049	-0.092	0.046	0.129	0.032	0.000	0.082	0.081	0.000	0.000
Total HREE	0.956	0.181	-0.069	0.163	-0.075	0.017	0.076	-0.012	0.094	-0.007	-0.031	0.024	0.000
Total LREE	0.849	-0.398	-0.275	-0.097	0.112	0.093	0.020	0.042	0.094	0.014	-0.052	-0.019	0.000
LREE/HREE	0.021	-0.812	-0.339	-0.336	0.268	0.158	-0.084	0.080	-0.025	-0.037	0.019	0.013	0.000

Contribution of the variables (%):

	F1	F2	F3	F4	F5	F6	F7	F8	F9	F10	F11	F12	F13
eNd(T)	0.596	25.935	5.563	1.087	6.887	5.575	2.432	49.970	0.852	0.927	0.000	0.173	0.002
SiO2	5.732	9.284	0.812	24.893	10.776	32.066	1.583	2.070	5.406	0.963	0.009	0.004	6.403
TiO2	12.447	2.474	2.461	0.401	0.595	6.878	16.840	13.033	6.612	32.123	1.127	2.545	2.465
Al2O3	9.981	6.806	0.034	2.989	9.264	0.214	35.927	4.460	3.997	2.958	13.663	1.610	8.097
FeOT	12.986	2.575	0.753	2.993	0.205	1.001	19.901	0.653	12.308	7.376	7.580	1.414	30.256
MgO	11.717	3.006	0.012	0.057	27.630	0.661	3.062	8.232	12.255	1.284	3.123	0.456	28.504
CaO	5.068	0.398	27.275	9.522	18.166	1.433	6.902	7.551	2.863	3.765	2.789	0.178	14.090
Total Alkalis	1.703	5.581	36.649	5.120	7.128	3.472	0.416	2.438	10.358	10.137	7.261	0.267	9.471
Total LILE	0.077	14.139	12.825	32.436	0.006	37.509	0.345	1.541	0.507	0.563	0.020	0.031	0.001
Total HFS	14.112	0.474	2.323	0.327	1.666	0.655	7.003	1.116	0.000	32.356	39.924	0.003	0.042
Total HREE	14.290	1.130	0.276	3.611	1.103	0.094	2.452	0.142	21.562	0.204	5.943	48.857	0.336
Total LREE	11.283	5.463	4.372	1.266	2.450	2.698	0.164	1.901	21.785	0.888	16.392	31.081	0.258
LREE/HREE	0.007	22.736	6.646	15.298	14.124	7.744	2.974	6.895	1.494	6.456	2.170	13.382	0.076

Squared cosines of the variables:

	F1	F2	F3	F4	F5	F6	F7	F8	F9	F10	F11	F12	F13
eNd(T)	0.038	**0.752**	0.096	0.008	0.035	0.018	0.006	0.047	0.000	0.000	0.000	0.000	0.000
SiO2	**0.366**	0.269	0.014	0.184	0.055	0.104	0.004	0.002	0.002	0.000	0.000	0.000	0.000
TiO2	**0.796**	0.072	0.043	0.003	0.003	0.022	0.040	0.012	0.003	0.007	0.000	0.000	0.000
Al2O3	**0.638**	0.197	0.001	0.022	0.047	0.001	0.086	0.004	0.002	0.001	0.002	0.000	0.000
FeOT	**0.830**	0.075	0.013	0.022	0.001	0.003	0.047	0.001	0.005	0.002	0.001	0.000	0.000
MgO	**0.749**	0.087	0.000	0.000	0.140	0.002	0.007	0.008	0.005	0.000	0.001	0.000	0.000
CaO	0.324	0.012	**0.471**	0.070	0.092	0.005	0.016	0.007	0.001	0.001	0.000	0.000	0.000
Total Alkalis	0.109	0.162	**0.633**	0.038	0.036	0.011	0.001	0.002	0.004	0.002	0.001	0.000	0.000
Total LILE	0.005	**0.410**	0.222	0.240	0.000	0.121	0.001	0.001	0.000	0.000	0.000	0.000	0.000
Total HFS	**0.902**	0.014	0.040	0.002	0.008	0.002	0.017	0.001	0.000	0.007	0.007	0.000	0.000
Total HREE	**0.913**	0.033	0.005	0.027	0.006	0.000	0.006	0.000	0.009	0.000	0.001	0.001	0.000
Total LREE	**0.721**	0.158	0.076	0.009	0.012	0.009	0.000	0.002	0.009	0.000	0.003	0.000	0.000
LREE/HREE	0.000	**0.659**	0.115	0.113	0.072	0.025	0.007	0.006	0.001	0.001	0.000	0.000	0.000

Values in bold correspond for each variable to the factor for which the squared cosine is the largest

Factor scores:

Observation	F1	F2	F3	F4	F5	F6	F7	F8	F9	F10	F11	F12	F13
F1001-32	-3.583	1.454	-0.699	-0.007	0.988	-0.138	0.166	-0.389	-0.072	0.103	0.099	-0.041	-0.004
F1001-36	-3.203	1.256	-0.296	-0.324	0.685	0.478	-0.667	-0.151	0.002	-0.065	0.097	-0.031	0.003
J1106-295.5	0.698	2.670	2.081	-1.453	0.234	0.484	0.848	0.521	-0.227	-0.048	-0.040	-0.016	0.002
J1106-193.2	0.554	1.136	1.830	-1.188	0.485	-0.389	-0.018	-0.439	0.292	0.142	0.178	0.043	-0.004
J1106-15.9	-2.139	-1.221	0.124	-0.425	-1.515	-0.622	0.224	-0.324	-0.287	-0.072	0.065	-0.016	0.001
F1142-110	1.357	0.417	-1.372	1.004	0.230	-0.841	1.100	0.374	0.164	-0.119	0.111	-0.014	-0.004
J1106-238	-0.309	3.110	0.592	0.489	-1.531	0.530	-0.481	0.393	0.085	0.040	0.097	0.039	0.000
J1106-93.7	-0.761	-2.015	2.225	1.620	0.303	0.163	-0.155	0.078	-0.045	-0.007	0.117	-0.040	0.010
F1142-77	1.545	0.157	-1.079	0.214	-0.339	-0.270	-0.616	0.351	0.246	0.015	0.125	-0.061	-0.003
F1001-13.5	-3.102	1.185	-0.623	0.071	0.220	-0.022	-0.071	-0.007	-0.265	0.025	-0.257	-0.012	-0.003
J1106-16.9	-1.808	-1.633	-0.273	-0.626	-1.134	-0.088	0.156	-0.278	0.024	-0.163	0.072	0.032	0.001
F1142-101	2.901	0.203	0.215	0.811	-0.190	-0.747	-0.541	0.014	-0.449	0.100	-0.039	0.012	-0.006
J1106-93.9	-0.799	-2.344	1.857	1.184	0.496	0.590	-0.005	0.116	0.015	0.139	-0.043	0.043	-0.007
J1106-107.6	0.889	-3.035	0.647	-0.681	-0.278	0.933	0.278	-0.054	0.155	-0.150	-0.105	-0.039	-0.007
F1142-88	2.264	-0.447	0.811	0.110	0.566	-0.873	0.410	-0.137	0.023	0.010	-0.066	0.026	0.008
F1001-49	-1.473	-1.143	-2.070	-0.277	1.107	0.201	-0.349	0.337	-0.116	-0.264	0.078	0.073	0.001
F1001-16	-3.202	1.494	-0.573	1.019	-0.399	-0.108	0.217	-0.148	0.393	0.015	-0.293	0.016	0.003
F1001-70	0.755	-1.978	-2.596	-0.785	-0.238	0.537	0.375	0.166	-0.040	0.439	0.028	0.005	0.005
J1106-138.8	2.552	-0.988	0.387	-1.405	0.235	-0.761	-0.894	0.202	0.165	-0.023	-0.198	-0.017	0.002
F622	6.864	1.725	-1.185	0.650	0.074	0.943	0.026	-0.625	-0.063	-0.115	-0.025	-0.002	0.002

Contribution of the observations (%):

	F1	F2	F3	F4	F5	F6	F7	F8	F9	F10	F11	F12	F13
F1001-32	10.042	3.647	1.415	0.000	9.612	0.295	0.577	8.071	0.627	2.543	2.953	7.351	3.360
F1001-36	8.023	2.720	0.253	0.710	4.619	3.538	9.351	1.210	0.000	1.017	2.861	4.130	2.324
J1106-295.5	0.381	12.303	12.525	14.281	0.540	3.625	15.077	14.499	6.303	0.567	0.488	1.051	1.033
J1106-193.2	0.240	2.225	9.685	9.540	2.321	2.345	0.007	10.291	10.397	4.887	9.572	7.873	3.848
J1106-15.9	3.577	2.573	0.045	1.220	22.619	5.990	1.052	5.586	10.085	1.264	1.293	1.108	0.352
F1142-110	1.440	0.301	5.449	6.811	0.520	10.933	25.408	7.459	3.291	3.426	3.700	0.809	4.338
J1106-238	0.075	16.687	1.013	1.618	23.096	4.337	4.861	8.247	0.882	0.386	2.834	6.495	0.035
J1106-93.7	0.453	7.008	14.324	17.741	0.904	0.409	0.507	0.325	0.244	0.010	4.173	6.902	22.807
F1142-77	1.868	0.042	3.370	0.309	1.135	1.124	7.962	6.571	7.399	0.054	4.710	16.140	2.443
F1001-13.5	7.528	2.422	1.123	0.034	0.479	0.007	0.107	0.003	8.571	0.146	20.028	0.666	2.217
J1106-16.9	2.557	4.599	0.215	2.652	12.667	0.119	0.513	4.129	0.071	6.443	1.572	4.336	0.080
F1142-101	6.583	0.071	0.134	4.453	0.354	8.625	6.150	0.010	24.612	2.403	0.469	0.663	8.771
J1106-93.9	0.499	9.483	9.982	9.479	2.426	5.385	0.001	0.716	0.028	4.668	0.567	7.873	12.110
J1106-107.6	0.618	15.895	1.210	3.138	0.763	13.478	1.619	0.156	2.944	5.434	3.341	6.521	11.483
F1142-88	4.009	0.345	1.902	0.081	3.151	11.793	3.523	1.007	0.063	0.023	1.324	2.926	14.170
F1001-49	1.698	2.256	12.403	0.520	12.075	0.626	2.555	6.048	1.635	16.815	1.851	22.751	0.487
F1001-16	8.019	3.853	0.950	7.028	1.564	0.182	0.991	1.173	18.857	0.057	25.947	1.093	2.255
F1001-70	0.445	6.753	19.506	4.169	0.557	4.462	2.945	1.469	0.193	46.515	0.242	0.116	5.914
J1106-138.8	5.095	1.686	0.432	13.355	0.545	8.966	16.781	2.187	3.307	0.132	11.886	1.187	1.100
F622	36.850	5.131	4.066	2.861	0.054	13.758	0.014	20.842	0.490	3.210	0.190	0.010	0.873

Squared cosines of the observations:

	F1	F2	F3	F4	F5	F6	F7	F8	F9	F10	F11	F12	F13
F1001-32	**0.771**	0.127	0.029	0.000	0.059	0.001	0.002	0.009	0.000	0.001	0.001	0.000	0.000
F1001-36	**0.777**	0.119	0.007	0.008	0.036	0.017	0.034	0.002	0.000	0.000	0.001	0.000	0.000
J1106-295.5	0.032	**0.463**	0.281	0.137	0.004	0.015	0.047	0.018	0.003	0.000	0.000	0.000	0.000
J1106-193.2	0.043	0.182	**0.473**	0.199	0.033	0.021	0.000	0.027	0.012	0.003	0.004	0.000	0.000
J1106-15.9	**0.498**	0.162	0.002	0.020	0.250	0.042	0.005	0.011	0.009	0.001	0.000	0.000	0.000
F1142-110	0.260	0.025	**0.266**	0.142	0.007	0.100	0.171	0.020	0.004	0.002	0.002	0.000	0.000
J1106-238	0.007	**0.722**	0.026	0.018	0.175	0.021	0.017	0.012	0.001	0.000	0.001	0.000	0.000
J1106-93.7	0.047	0.328	**0.400**	0.212	0.007	0.002	0.002	0.000	0.000	0.000	0.001	0.000	0.000
F1142-77	**0.544**	0.006	0.265	0.010	0.026	0.017	0.086	0.028	0.014	0.000	0.004	0.001	0.000
F1001-13.5	**0.829**	0.121	0.033	0.000	0.004	0.000	0.000	0.000	0.006	0.000	0.006	0.000	0.000
J1106-16.9	**0.417**	0.340	0.009	0.050	0.164	0.001	0.003	0.010	0.000	0.003	0.001	0.000	0.000
F1142-101	**0.820**	0.004	0.005	0.064	0.004	0.054	0.029	0.000	0.020	0.001	0.000	0.000	0.000
J1106-93.9	0.055	**0.473**	0.297	0.121	0.021	0.030	0.000	0.001	0.000	0.002	0.000	0.000	0.000
J1106-107.6	0.066	**0.769**	0.035	0.039	0.006	0.073	0.006	0.000	0.002	0.002	0.001	0.000	0.000
F1142-88	**0.705**	0.028	0.090	0.002	0.044	0.105	0.023	0.003	0.000	0.000	0.001	0.000	0.000
F1001-49	0.230	0.139	**0.454**	0.008	0.130	0.004	0.013	0.012	0.001	0.007	0.001	0.001	0.000
F1001-16	**0.715**	0.156	0.023	0.072	0.011	0.001	0.003	0.002	0.011	0.000	0.006	0.000	0.000
F1001-70	0.045	0.312	**0.537**	0.049	0.005	0.023	0.011	0.002	0.000	0.015	0.000	0.000	0.000
J1106-138.8	**0.584**	0.088	0.013	0.177	0.005	0.052	0.072	0.004	0.002	0.000	0.004	0.000	0.000
F622	**0.885**	0.056	0.026	0.008	0.000	0.017	0.000	0.007	0.000	0.000	0.000	0.000	0.000

Values in bold correspond for each observation to the factor for which the squared cosine is the largest

Table DR2. LA-ICP-MS U-Pb geochronologic analyses of sample F6248

	Isotope ratios									Apparent ages (Ma)							
	U (ppm)	206Pb/204Pb	U/Th	206Pb*/207Pb*	± (%)	207Pb*/235U*	± (%)	206Pb*/238U*	± (%)	error corr.	206Pb*/238U*	±	207Pb*/235U	±	206Pb*/207Pb*	±	Best age	±	Conc (%)
F6248-7 <>	85	81899	2.1	5.1399	0.3	14.3609	0.8	0.5353	0.7	0.90	2763.9	15.4	2773.8	7.3	2781.1	5.6	2781.1	5.6	99.4
F6248-34 <>	127	103824	3.7	6.3544	0.8	9.9952	3.4	0.4606	3.3	0.97	2442.4	66.4	2434.3	31.1	2427.6	13.6	2427.6	13.6	100.6
F6248-20 <>	252	27797	3.7	6.9720	3.1	6.9675	4.6	0.3523	3.4	0.74	1945.6	57.5	2107.3	41.0	2269.0	53.3	2269.0	53.3	85.7
F6248-21 <>	52	91746	1.0	8.5319	1.2	5.4716	1.4	0.3386	0.7	0.48	1879.8	10.8	1896.1	11.8	1914.0	21.5	1914.0	21.5	98.2
F6248-86 <>	115	55487	1.8	8.9415	0.7	4.9444	2.0	0.3206	1.8	0.93	1792.9	28.9	1809.9	16.8	1829.5	13.5	1829.5	13.5	98.0
F6248-39 <>	179	80714	2.1	10.7651	0.6	3.3161	6.5	0.2589	6.4	1.00	1484.2	85.4	1484.8	50.6	1485.7	11.9	1485.7	11.9	99.9
F6248-61 <>	156	143669	1.6	10.8011	0.7	3.1372	1.2	0.2458	1.0	0.85	1416.6	13.3	1441.9	9.5	1479.4	12.4	1479.4	12.4	95.8
F6248-23 <>	174	114308	3.3	10.8512	0.5	3.2920	0.9	0.2591	0.8	0.87	1485.1	10.8	1479.2	7.3	1470.6	8.9	1470.6	8.9	101.0
F6248-97 <>	510	31340	1.4	11.4000	0.5	2.7074	1.8	0.2238	1.7	0.97	1302.2	20.1	1330.5	13.1	1376.3	8.9	1376.3	8.9	94.6
F6248-94 <>	245	29691	2.2	11.4180	0.4	2.7655	1.7	0.2290	1.6	0.97	1329.4	19.4	1346.3	12.4	1373.3	7.8	1373.3	7.8	96.8
F6248-76 <>	146	76194	2.6	11.6928	1.1	2.4397	3.3	0.2069	3.1	0.94	1212.3	34.4	1254.4	23.8	1327.4	21.8	1327.4	21.8	91.3
F6248-10 <>	142	60042	2.8	11.7792	0.6	2.6215	2.6	0.2240	2.5	0.97	1302.7	29.6	1306.7	19.0	1313.1	12.4	1313.1	12.4	99.2
F6248-83 <>	79	6149	1.6	11.8608	2.9	2.5643	3.9	0.2206	2.6	0.66	1285.0	29.9	1290.5	28.3	1299.7	56.5	1299.7	56.5	98.9
F6248-18 <>	84	75661	3.9	12.3406	1.4	2.1372	2.1	0.1913	1.5	0.73	1128.3	15.7	1160.9	14.4	1222.2	28.1	1222.2	28.1	92.3
F6248-64 <>	60	40006	1.2	13.3348	2.2	1.9146	2.6	0.1852	1.4	0.53	1095.2	13.9	1086.2	17.5	1068.3	44.8	1068.3	44.8	102.5
F6248-74 <>	174	115947	1.7	13.4429	1.4	1.7711	1.9	0.1727	1.3	0.70	1026.8	12.5	1034.9	12.3	1052.1	27.4	1052.1	27.4	97.6
F6248-15 <>	126	31027	2.6	14.8488	2.7	1.1826	3.5	0.1274	2.3	0.66	772.8	17.0	792.5	19.5	848.5	55.5	772.8	17.0	91.1
F6248-29 <>	91	20220	2.2	15.8086	2.0	1.0780	2.8	0.1236	2.0	0.72	751.2	14.5	742.6	15.0	716.9	41.8	751.2	14.5	104.8
F6248-88 <>	63	1997	1.9	15.3531	5.5	1.1068	6.0	0.1232	2.4	0.39	749.2	16.7	756.6	32.1	778.6	116.2	749.2	16.7	96.2
F6248-67 <>	81	3003	1.6	15.1233	6.3	1.1046	6.4	0.1212	1.4	0.22	737.2	9.7	755.6	34.3	810.3	131.7	737.2	9.7	91.0
F6248-36 <>	140	48560	2.1	15.6745	3.2	1.0656	3.4	0.1211	1.2	0.36	737.1	8.5	736.6	18.0	735.0	68.1	737.1	8.5	100.3
F6248-41 <>	118	46003	1.8	15.7424	2.6	1.0564	3.1	0.1206	1.7	0.55	734.1	12.0	732.0	16.4	725.8	55.4	734.1	12.0	101.1
F6248-32 <>	113	30447	2.0	15.8948	1.5	1.0432	1.8	0.1203	1.1	0.59	732.1	7.5	725.5	9.4	705.3	31.1	732.1	7.5	103.8
F6248-27 <>	125	40044	2.8	15.7980	2.1	1.0479	2.6	0.1201	1.5	0.58	730.9	10.5	727.8	13.6	718.3	45.3	730.9	10.5	101.8
F6248-40 <>	166	8857	2.1	15.6866	2.9	1.0544	3.2	0.1200	1.3	0.42	730.3	9.2	731.1	16.7	733.3	61.5	730.3	9.2	99.6
F6248-78 <>	111	46856	2.9	15.4994	1.8	1.0669	2.8	0.1199	2.0	0.74	730.2	14.1	737.2	14.4	758.7	38.7	730.2	14.1	96.2
F6248-48 <>	156	29604	2.0	15.6206	1.0	1.0587	1.3	0.1199	0.9	0.66	730.2	6.0	733.2	6.9	742.2	21.2	730.2	6.0	98.4
F6248-55 <>	112	28056	1.9	15.7004	2.7	1.0513	3.3	0.1197	1.8	0.55	728.9	12.4	729.5	17.0	731.5	57.8	728.9	12.4	99.7
F6248-30 <>	87	35528	2.0	15.7008	5.0	1.0507	5.1	0.1196	1.1	0.21	728.5	7.3	729.2	26.4	731.4	105.3	728.5	7.3	99.6
F6248-12 <>	126	21521	1.9	14.8909	2.8	1.1078	4.7	0.1196	3.8	0.80	728.5	25.8	757.1	25.0	842.6	58.4	728.5	25.8	86.5
F6248-37 <>	187	6261	1.5	15.6151	1.6	1.0559	1.9	0.1196	1.0	0.53	728.2	6.9	731.8	9.8	742.9	33.6	728.2	6.9	98.0
F6248-70 <>	139	3919	3.3	15.2994	4.5	1.0772	5.0	0.1195	2.1	0.42	727.8	14.6	742.2	26.3	786.0	95.2	727.8	14.6	92.6
F6248-31 <>	131	17069	1.7	15.7006	2.3	1.0491	2.5	0.1195	0.9	0.36	727.4	6.1	728.4	12.8	731.4	48.5	727.4	6.1	99.5
F6248-54 <>	111	15143	2.5	15.7379	2.9	1.0455	3.2	0.1193	1.4	0.43	726.8	9.3	726.7	16.5	726.4	60.9	726.8	9.3	100.1
F6248-50 <>	127	22348	2.4	15.4125	2.1	1.0662	2.4	0.1192	1.2	0.50	725.8	8.3	736.9	12.6	770.5	43.9	725.8	8.3	94.2
F6248-73 <>	85	15289	1.9	15.8995	3.5	1.0333	3.7	0.1192	1.4	0.37	725.7	9.4	720.6	19.2	704.7	73.8	725.7	9.4	103.0
F6248-65 <>	103	18399	1.8	15.6781	4.4	1.0477	4.6	0.1191	1.4	0.31	725.6	9.9	727.8	24.1	734.5	93.2	725.6	9.9	98.8
F6248-22 <>	52	783	2.9	14.9687	4.7	1.0973	4.8	0.1191	1.3	0.28	725.5	9.3	752.1	25.8	831.8	97.1	725.5	9.3	87.2
F6248-31 <>	176	40867	2.6	15.9246	2.1	1.0294	2.4	0.1189	1.0	0.42	724.2	6.7	718.6	12.1	701.3	45.5	724.2	6.7	103.3
F6248-52 <>	100	72521	2.3	15.8627	3.8	1.0324	4.3	0.1188	2.2	0.50	723.5	14.8	720.1	22.4	709.6	80.1	723.5	14.8	102.0
F6248-66 <>	80	3118	2.0	15.5952	5.1	1.0496	5.3	0.1187	1.4	0.26	723.2	9.5	728.7	27.4	745.6	107.6	723.2	9.5	97.0
F6248-4 <>	132	68061	3.0	15.5149	2.9	1.0544	3.1	0.1186	1.0	0.32	722.7	6.9	731.0	16.2	756.6	62.1	722.7	6.9	95.5
F6248-71 <>	149	4023	1.1	15.5286	2.7	1.0531	3.4	0.1186	2.0	0.60	722.5	14.0	730.4	17.6	754.7	57.0	722.5	14.0	95.7
F6248-28 <>	149	40214	1.7	15.9114	2.7	1.0274	2.8	0.1186	0.6	0.21	722.3	4.0	717.6	14.3	703.1	58.0	722.3	4.0	102.7
F6248-45 <>	256	69452	1.4	15.6990	1.3	1.0412	1.6	0.1185	0.8	0.53	722.2	5.7	724.5	8.2	731.6	28.2	722.2	5.7	98.7
F6248-25 <>	145	49449	2.5	15.6875	1.8	1.0404	1.8	0.1184	0.5	0.29	721.2	3.6	724.1	9.5	733.2	37.2	721.2	3.6	98.4
F6248-51 <>	151	85107	1.9	15.8900	2.7	1.0260	2.9	0.1182	0.9	0.31	720.4	6.1	716.9	14.8	705.9	58.1	720.4	6.1	102.1
F6248-47 <>	135	43619	1.8	16.0383	2.7	1.0164	2.8	0.1182	1.0	0.34	720.3	6.5	712.1	14.5	686.2	56.9	720.3	6.5	105.0
F6248-69 <>	120	44092	2.9	15.4410	2.3	1.0555	2.6	0.1182	1.2	0.45	720.2	8.1	731.6	13.7	766.6	49.3	720.2	8.1	93.9
F6248-19 <>	115	28838	3.3	15.7058	1.6	1.0358	1.8	0.1180	0.9	0.49	719.0	6.1	721.8	9.4	730.7	33.4	719.0	6.1	98.4
F6248-13 <>	154	31232	3.3	15.5457	1.8	1.0451	2.0	0.1178	1.0	0.49	718.1	6.8	726.5	10.6	752.4	37.7	718.1	6.8	95.4
F6248-24 <>	93	28996	2.3	15.6961	2.4	1.0348	2.8	0.1178	1.5	0.54	717.9	10.4	721.3	14.7	732.0	50.6	717.9	10.4	98.1

Table S2 cont. LA-ICP-MS U-Pb geochronologic analyses of sample F6248

	Isotope ratios									Apparent ages (Ma)							
	U (ppm)	206Pb/204Pb	U/Th	206Pb*/207Pb*	± (%)	207Pb*/235U*	± (%)	206Pb*/238U*	± (%)	error corr.	206Pb*/238U*	±	207Pb*/235U	±	206Pb*/207Pb*	±	Best age	±	Conc (%)

Table DR3. CA-TIMS U-Th-Pb isotopic data of selceted grains from sample F6248

		Compositional Parameters						Radiogenic Isotope Ratios								Isotopic Ages						LA-ICPMS results			
TIMS#	LA#	Th/U	$^{206}Pb^*$ x10^{-13} mol	mol % $^{206}Pb^*$	Pb^*/Pb_c	Pb_c (pg)	$^{206}Pb/^{204}Pb$	$^{208}Pb/^{206}Pb$	$^{207}Pb/^{206}Pb$	% err	$^{207}Pb/^{235}U$	% err	$^{206}Pb/^{238}U$	% err	corr. coef.	$^{207}Pb/^{206}Pb$	±	$^{207}Pb/^{235}U$	±	$^{206}Pb/^{238}U$	±	$^{206}Pb/^{238}U$	± (1s)	U (ppm)	Th/U
(a)	(a)	(b)	(c)	(c)	(c)	(c)	(d)	(e)	(e)	(f)	(e)	(f)	(e)	(f)		(g)	(f)	(g)	(f)	(g)	(f)				
F6248																									
z7	75	0.312	0.4420	99.49%	56	0.19	3522	0.096	0.063555	0.122	1.040642	0.183	0.118809	0.083	0.835	725.89	2.59	724.24	0.95	723.70	0.57	717	15	155	0.4545
z5	53	0.584	0.8454	99.57%	72	0.30	4226	0.180	0.063741	0.105	1.043224	0.160	0.118755	0.071	0.857	732.10	2.22	725.52	0.83	723.39	0.49	714	12	113	0.5263
z8	91	0.317	0.1868	98.37%	17	0.26	1107	0.098	0.063404	0.323	1.032681	0.388	0.118181	0.144	0.599	720.84	6.85	720.27	2.00	**720.08**	**0.98**	697	9	237	0.4348
z6	70	0.343	0.4704	99.33%	43	0.26	2683	0.106	0.063534	0.145	1.034016	0.202	0.118090	0.089	0.773	725.21	3.07	720.93	1.04	**719.56**	**0.61**	728	15	139	0.30
z4	37	0.600	0.3077	98.61%	22	0.36	1300	0.186	0.063425	0.275	1.032237	0.328	0.118090	0.104	0.625	721.56	5.84	720.05	1.69	**719.56**	**0.71**	728	7	187	0.6667
z1	4	0.322	0.4582	99.38%	46	0.24	2898	0.100	0.063360	0.149	1.031020	0.207	0.118072	0.094	0.755	719.37	3.16	719.44	1.07	**719.46**	**0.64**	723	7	132	0.3333
z2	17	0.621	0.6039	99.48%	60	0.26	3484	0.192	0.063466	0.116	1.032535	0.220	0.118048	0.157	0.862	722.92	2.46	720.19	1.13	**719.32**	**1.07**	700	6	122	0.5556
z3	24	0.584	0.5890	99.43%	54	0.28	3158	0.181	0.063528	0.131	1.033330	0.187	0.118024	0.082	0.791	724.99	2.79	720.59	0.96	**719.18**	**0.56**	718	10	93	0.4348

(a) TIMS# corresponds to the annealed, chemically abraded, and dissolved partial grain with corresponding laser spot analysis given by LA#.
(b) Model Th/U ratio iteratively calculated from the radiogenic 208Pb/206Pb ratio and 206Pb/238U age.
(c) Pb* and Pbc represent radiogenic and common Pb, respectively; mol % $^{206}Pb^*$ with respect to radiogenic, blank and initial common Pb.
(d) Measured ratio corrected for spike and fractionation only. Fractionation estimated at 0.16 +/- 0.03 %/a.m.u. for Daly analyses, based on analysis of NBS-981 and NBS-982.
(e) Corrected for fractionation, spike, and common Pb; all was assumed to be procedural blank: 206Pb/204Pb = 18.042 ± 0.61%; 207Pb/204Pb = 15.537 ± 0.52%; 208Pb/204Pb = 37.686 ± 0.63% (all uncertainties 1-sigma).
(f) Errors are 2-sigma, propagated using the algorithms of Schmitz and Schoene (2007).
(g) Calculations are based on the decay constants of Jaffey et al. (1971). 206Pb/238U and 207Pb/206Pb ages corrected for initial disequilibrium in 230Th/238U using Th/U [magma] = 3.
(h) Corrected for fractionation, spike, and blank Pb only.

Weighted Mean on bold analyses (6 youngest)

$^{206}Pb/^{238}U$ ± random (+tracer) [+l]		MSWD	prob. fit
719.47 ± 0.29 (0.44) [0.86]	**± 2s int.**	**0.57**	0.989
		n =	6

F6248-62 <>	157	14944	1.8	15.0455	4.1	1.0795	4.7	0.1178	2.3	0.48	717.9	15.3	743.4	24.7	821.1	85.8	717.9	15.3	87.4
F6248-99 <>	94	2556	1.5	15.0276	3.1	1.0795	3.8	0.1177	2.1	0.56	717.1	14.4	743.4	19.9	823.6	65.1	717.1	14.4	87.1
F6248-75 <>	155	78166	2.2	15.7390	2.4	1.0301	3.2	0.1176	2.2	0.69	716.6	15.2	719.0	16.7	726.2	49.9	716.6	15.2	98.7
F6248-79 <>	139	8907	1.8	15.3443	3.2	1.0553	3.8	0.1174	2.0	0.54	715.8	13.9	731.5	19.7	779.8	66.9	715.8	13.9	91.8
F6248-42 <>	99	28361	1.7	16.0085	3.0	1.0113	3.3	0.1174	1.5	0.44	715.7	9.9	709.5	16.8	690.1	63.1	715.7	9.9	103.7
F6248-46 <>	69	7784	2.4	15.2571	6.2	1.0593	6.2	0.1172	0.6	0.10	714.5	4.2	733.5	32.3	791.8	129.1	714.5	4.2	90.2
F6248-53 <>	113	20093	1.9	15.4874	2.5	1.0433	3.1	0.1172	1.8	0.59	714.3	12.2	725.5	15.9	760.3	52.2	714.3	12.2	94.0
F6248-3 <>	168	43615	2.0	15.8610	1.5	1.0180	2.1	0.1171	1.4	0.68	713.9	9.7	712.9	10.8	709.9	32.8	713.9	9.7	100.6
F6248-81 <>	190	26729	1.8	15.6920	2.2	1.0276	2.5	0.1169	1.2	0.47	713.0	7.9	717.7	12.8	732.6	46.3	713.0	7.9	97.3
F6248-56 <>	142	47805	1.9	15.7768	2.9	1.0215	3.0	0.1169	0.6	0.22	712.6	4.3	714.7	15.2	721.1	61.2	712.6	4.3	98.8
F6248-6 <>	135	47904	2.0	15.7476	1.5	1.0224	2.1	0.1168	1.5	0.71	711.9	10.3	715.1	10.9	725.1	31.6	711.9	10.3	98.2
F6248-80 <>	99	9670	1.9	15.0229	8.5	1.0706	9.1	0.1167	3.3	0.36	711.3	22.4	739.1	47.9	824.2	177.4	711.3	22.4	86.3
F6248-89 <>	163	49017	2.0	15.9157	2.2	1.0100	3.7	0.1166	3.0	0.81	710.9	20.2	708.9	19.0	702.5	46.8	710.9	20.2	101.2
F6248-2 <>	119	44358	3.3	15.7739	3.0	1.0190	3.4	0.1166	1.6	0.46	710.8	10.6	713.4	17.4	721.5	63.7	710.8	10.6	98.5
F6248-14 <>	134	35946	2.9	15.9153	1.8	1.0075	2.1	0.1163	1.1	0.50	709.2	7.1	707.6	10.8	702.6	39.0	709.2	7.1	100.9
F6248-58 <>	147	12080	3.2	15.5079	2.7	1.0323	2.9	0.1161	1.1	0.38	708.1	7.4	720.1	14.9	757.5	56.3	708.1	7.4	93.5
F6248-77 <>	90	11989	1.7	15.9777	1.9	1.0015	2.6	0.1161	1.8	0.69	707.8	11.9	704.6	13.1	694.2	40.0	707.8	11.9	102.0
F6248-1 <>	128	19190	2.5	16.0664	1.5	0.9955	2.0	0.1160	1.3	0.66	707.5	8.8	701.5	10.2	682.4	32.4	707.5	8.8	103.7
F6248-9 <>	113	56333	2.2	15.3177	4.5	1.0430	5.1	0.1159	2.5	0.48	706.8	16.6	725.4	26.6	783.5	94.4	706.8	16.6	90.2
F6248-49 <>	90	2311	1.9	14.7115	6.3	1.0852	6.8	0.1158	2.6	0.38	706.3	17.3	746.2	35.9	867.8	130.3	706.3	17.3	81.4
F6248-85 <>	194	60006	2.9	15.9064	1.0	1.0023	2.3	0.1156	2.0	0.89	705.3	13.6	705.0	11.6	703.8	21.7	705.3	13.6	100.2
F6248-67 <>	104	19489	1.6	15.7227	3.3	1.0129	3.6	0.1155	1.4	0.38	704.6	9.0	710.3	18.2	728.5	69.9	704.6	9.0	96.7
F6248-100 <>	85	53426	2.3	15.8537	4.7	1.0045	5.1	0.1155	1.7	0.34	704.6	11.5	706.1	25.7	710.8	101.0	704.6	11.5	99.1
F6248-95 <>	213	130549	2.5	15.8678	1.2	1.0016	1.6	0.1153	1.1	0.68	703.3	7.2	704.6	8.1	708.9	24.7	703.3	7.2	99.2
F6248-96 <>	107	31575	1.5	15.5304	2.2	1.0192	2.6	0.1148	1.3	0.51	700.6	8.7	713.5	13.2	754.4	46.6	700.6	8.7	92.9
F6248-11 <>	85	41082	2.8	15.7146	2.8	1.0068	3.0	0.1147	1.3	0.42	700.3	8.5	707.3	15.5	729.5	58.4	700.3	8.5	96.0
F6248-17 <>	122	56840	1.8	15.7235	2.4	1.0055	2.6	0.1147	0.9	0.34	699.8	5.8	706.6	13.1	728.3	51.3	699.8	5.8	96.1
F6248-91 <>	237	106106	2.3	15.6991	1.5	1.0033	2.0	0.1142	1.3	0.66	697.3	8.6	705.5	10.1	731.6	31.5	697.3	8.6	95.3